University of Texas at El Paso

ScholarWorks@UTEP

2023-05-01

Development Of Multi-Configuration Methods On Density Functional Theory Orbitals And Application On The Study Of Dimers

Jose Gustavo Bravo Flores
University of Texas at El Paso

DEVELOPMENT OF MULTI-CONFIGURATION METHODS

ON DENSITY FUNCTIONAL THEORY ORBITALS

AND APPLICATION ON THE STUDY OF DIMERS

JOSE GUSTAVO BRAVO FLORES, B. S.

Master's Program in Physics

APPROVED:

_____
 Mark R. Pederson, Ph.D., Chair

_____
Koblar A. Jackson, Ph.D., Co-Chair

_____
Jorge A. Munoz, Ph.D.

_____
Stephen L. Crites, Jr., Ph.D.
Dean of the Graduate School

to my sisters
Sofia and Aurora

DEVELOPMENT OF MULTI-CONFIGURATION METHODS

ON DENSITY FUNCTIONAL THEORY ORBITALS

AND APPLICATION ON THE STUDY OF DIMERS

by

JOSE GUSTAVO BRAVO FLORES, B. S.

THESIS

Presented to the Faculty of the Graduate School of

The University of Texas at El Paso

in Partial Fulfillment

of the Requirements

for the Degree of

MASTER OF SCIENCE

Department of Physics

THE UNIVERSITY OF TEXAS AT EL PASO

May 2023

Acknowledgements

I would like to thank my advisors, Dr Mark R. Pederson and Dr Koblar A. Jackson, for their support, guidance and discussion. They not only taught me how to be a better researcher, but a better person, showing me the kindness and real meaning of doing science.[1] I also want to thank Dr Jorge A. Munoz for serving on my committee, the many discussions about academia, research and promoting the inclusion of hispanics in science. A special thanks to Dr Kushantha Withanage and Mr. Alex Johnson (MS), for their immense patience while teaching me about programming and density functional theory, as well as making my stay in the laboratory the most enjoyable.

Finally, I want to give the biggest thanks to my family; my parents and sisters, for being there for me at all times, supporting my decisions and inspiring me into becoming a better person. I could not have asked for more, it is due to them that I have come so far.

---

[1]I still can't distinguish between a "C" and a "Z" when they are spelling.

Abstract

The configuration interaction (CI) methods is an exact method to solve the non relativistic Schrodinger equation, describing the wave function as a linear combination of Slater determinants. Because the computation time grows factorially as the number of electrons, CI is mostly used for relatively small systems. Density functional theory (DFT) rose as one of the most used methods for computational quantum chemistry in the last 30 years. DFT can describe a system's properties with the electron density, which only depends of of three coordinates. Due to its low computational costs it allows one to study bigger systems than CI, however it does not have the same accuracy as the former. In this work we present a methodology to calculate the overlap between electron configurations that have different Kohn-Sham orbitals (KSO), where the KSO obtained from DFT are used to build Slater determinants, and the overlap of these is calculated as in CI. The overlap tool application is shown in the study of three different dimers, H_2, N_2, and Cr_2, to review the collapse phenomena of a polarized electron density into an indistinguishable unpolarized state. Our results show how the collapse of a polarized state into an unpolarized solution does not require a complete overlap.

Table of Contents

List of Figures

List of Tables

Chapter 1

Introduction

1.1 Quantum Mechanics

By the end of XIX century physicists were facing what are called, fundamental problems, in the sense that the existent physical theories available could not be used to analyze these problems, or the results obtained from them would be erroneous [1]. Among these problems we have the black body radiation and the ultraviolet catastrophe, Compton scattering, and the photoelectric effect. We will not attempt to solve any of these problems here, but instead, we will review their story, and the paradigm changes that came as a consequence.

In 1860, Gustav Kirchhoff defined a black body as a system of infinitely small thickness that completely absorbs all incident rays and neither reflects nor transmit any [2]. This theoretical system, although non existent in nature, is a very important concept to understand radiation emission and absorption. Almost 40 years later, Wilhelm Wien obtained a formula to describe the spectrum of thermal radiation of a blackbody, this formula is often referred as Wien's distribution law, unfortunately it only yields correct results at high frequencies [3]. In June of 1900 Lord Rayleigh derived an expression, using classical arguments, that would eventually be known, until 1905 with help of Sir James H. Jeans, as the Rayleigh–Jeans law, this formula failed to describe the blackbody radiation at high frequencies [4], and it gave birth to the ultraviolet catastrophe, a consequence of the classical approach to describe the spectrum of thermal radiation of the blackbody. In December of the same year, Max Planck derived what we know as Planck's radiation law, an indisputably correct formula that has a very important caveat, a blackbody can only change its energy in discrete amounts of energy, quantas of energy, proportional to the frequency of

the associated radiation, this law can be reduced to Wien's and Rayleigh formulas in the proper limits of the frequency [5]. Planck received the 1918 Nobel prize in physics.

Classical electrodynamics predicts that a continuous light wave transfers energy to the electrons on a material, and after accumulating enough energy, these electrons would be emitted, inconveniently, this is not the case, but in 1905, Albert Einstein showed that light can be considered "discrete packages", later referred to as "photons" by Gilbert N. Lewis, asides of the widely accepted wave theory of light, and that for an electron to be emitted from a material it must be struck by one of this packages with sufficient energy to release it from the material [6]. Einstein was awarded the 1921 Nobel in physics for his discovery of the law of the photoelectric effect. Arthur H. Compton showed in 1923 that when high energy light is scattered after colliding with an electron, the scattered light's energy depends on the scattering angle of the light particle, proving once again that light should be considered as a particle, aside of being a wave. In his experiment X-rays were used ($\approx 17\,\mathrm{keV}$) so that a graphite electrons can be considered free [7]. Compton received the 1927 Nobel prize in physics for his discovery of this effect that bears his name.

Louis de Broglie proposed, in his doctoral thesis in 1924, that matter should behave as a waves just as light behaves as a particle [8]. In 1927 Davisson and Germer showed that electrons scattered by a surface of a crystal display a diffraction pattern, confirming that matter does have undulatory properties [9]. de Broglie received the 1929 Nobel prize in physics

These discoveries are the grounds for what we know as quantum mechanics, from the discrete exchange of energy in radiation absorption to the corpuscular behaviour of light. These results are not minuscule, they led to years of scientific and technological advances.

1.1.1 Schrödinger Equation

Quantum mechanics, although successful in explaining many phenomena that classical mechanics failed to, was still a theory in development taking it first steps. In 1926, Erwin Schrödinger proposed in a paper a derivation of a wave equation, today known as

Schrödinger's equation, and used it to find the correct non-relativistic energy eigenvalues of Hydrogen-like atoms, where the quantization aspect came naturally on the solutions [10].

$$\hat{H}\,|\Psi\rangle = i\hbar\frac{d}{dt}\,|\Psi\rangle \ ^1 \tag{1.1}$$

$\hat{H}$ is the hamiltonian operator, which is made up of the different energies and interactions of the system to consider, for a hydrogen atom, for example, we would have; the kinetic energy of the nucleus, the kinetic energy of the electron, and the coulomb interaction between the electron and the nucleus. As more particles get involved, this terms grow bigger and the equation to solve becomes more complicated.

1.1.2   Born-Oppenheimer Approximation

As mentioned before in subsection 1.1.1, as the system grows in difficulty, so do the solutions, and solving the Schrödinger equation becomes, and usually is, impossible to do analytically. Consider a system like the benzene molecule where we have 12 nuclei with 42 electrons, this means that we have a total of 162 coordinates to solve the Schrödinger equation for, this is a huge number of coordinates to work with, even with computational tools.

In 1927, Max Born and Robert Oppenheimer proposed that due to the difference in mass of the electrons and nuclei, the later can be treated as fixed in space, and that their wave functions can be treated independently[11].

This approximation has great value in numerical methods, lets go back to our benzene example: if we use the Born-Oppenheimer approximation we reduce the problem from 162 to 126 coordinates, this does not look as much but the computational complexity of most numerical methods grows faster than the square of the number of coordinates.

---

[1]This notation was not used by Schrödinger, but developed by Paul Dirac to work on a the matrix formulation of quantum mechanics.

1.2   Density Functional Theory

As we have seen, solving the Schrödinger equation for a large system involves facing many issues regarding computational efficiency. There is a way to circle around this problem; lets consider that all the electrons in our system are altogether an electron gas, and that all the important properties of our system can be determined in terms of functionals that depend on the electron gas density. This method of working with quantum systems is known as Density Functional Theory (DFT). In the following sections we will discuss the most important parts of this method.

DFT is widely used not only by physicists, but by chemists and engineers, anyone who is interested in the electronic properties of materials knows and uses this theory, to certain extent.

1.2.1   Hohenberg-Kohn Theorem

The theorem that set the first stone for DFT to exist is the Hohenber-Kohn theorem, said theorem states that the ground state energy is a unique functional of the electron density [12]. Said density only depends on three coordinates.

$$E = E[\rho(\vec{r})] \tag{1.2}$$

So far, DFT has reduced our $3N$-dimensional problem into a 3-dimensional one. But what is the form of this magical functional? it is unknown, and must be approximated. Life is never good, is it?

1.2.2   Kohn-Sham Theory

In 1965, W. Kohn and L. J. Sham showed that the electron density that minimizes the ground state functional coincides with the true electron density, and that the problem can be simplified from the many body interacting Hamiltonian into an elegant non-interacting differential equation [13].

$$\left[\hat{T} + \hat{U}_Z + \hat{U}_H + \hat{U}_{XC}\right] |\psi_i\rangle = \epsilon_i |\psi_i\rangle \tag{1.3}$$

$\hat{T}$ is the kinetic energy, $\hat{U}_Z$ is the Coulomb interaction with the Nuclei, $\hat{U}_H$ is the Hartree potential, which considers the repulsion between a KS orbital and the total electron density, and $\hat{U}_{XC}$ is the exchange correlation (XC) potential, which is unknown and must be approximated.

Finding a suitable exchange correlation potential is a hard task that has been object of research for many scientists, and although nowadays we have access many different XC potentials, the fact that there is no systematic way to improve an XC potential, means that there is no guarantee that utilising a more complicated potential will be sufficient to obtain better results overall [14].

It is important to point out that the differential equations for the Kohn-Sham orbitals depend on the electron density that we are looking for, because of this, in order to find a solution, there must be an iterative process; proposing a test electron density a first set of Kohn Sham orbitals is obtained, from which a new electron density is calculated and then repeat these steps until self consistency is achieved.

1.2.3   Self Interaction Error

Looking back into eq 1.3 , it is clear that there is a nonphysical effect in our equation. If the Hartree potential describes the interaction between an electron and the total electron density, then this electron is interacting with itself, this is commonly known as self interaction error (SIE). Interesting enough this is not a problem of the Kohn-Sham theory, but of DFT ever since.

Chapter 2

Dimers, Coulson-Fischer Point and Overlaps

2.1 Dimers

A dimer is a molecule formed by two similar parts, either two same element atoms or two identical molecules. The most famous dimer could be O_2. Although conceptually simple, dimers are very interesting systems to study, there are many papers studying many different dimers with different computational approaches [15, 16, 17].

For two atoms to bond and form a dimer the shared electrons between the two parts must have different spins. Let's think about O_2 again: Oxygen's electron configuration is $1s^2 2s^2 2p^4$, because the 2p orbital fits 6 electrons, there are two electron spins not being occupied which must be occupied by the second Oxygen's outer electrons in order for a bond to exist. If both Oxygen's electrons occupy the same spin states, the highest occupied molecular orbitals (HOMOs) associated with the parallel-spin staes do not participate in bond formation. However, it is usually the case that orbitals below the HOMO level participate in bond formation.

2.1.1 Wave Mechanics Perspective

Far Away Atoms

For two atoms that are separated enough for each of them to not interact with the other's electrons, if the polarization of the atoms is unknown, the wave function may be expressed

as a superposition of all possible states with the same total M_s.

Lets consider a two unpaired electrons system for simplicity:

$$|UPO\rangle = \frac{1}{\sqrt{4}}\left(|\uparrow\rangle_a |\downarrow\rangle_a + |\uparrow\rangle_a |\downarrow\rangle_b + |\uparrow\rangle_b |\downarrow\rangle_a + |\uparrow\rangle_b |\downarrow\rangle_b\right) \qquad (2.1)$$

Where $|\uparrow\rangle_a$, and $|\downarrow\rangle_b$ is a spin up electron localized around atom a, and a spin down electron localized around atom b, respectively. Notice that, the second and third terms are the classical representation of two well separated atoms. The first and fourth highlight the inaccuracy in the stretch bond limit of single configuration composed of single particle orbitals constrained to be symmetric. These terms correspond to anionic and cationic pairs of atoms, or a zwitter ion configuration. In condensed matter physics these configurations are also known as the upper Hubbard band. If we want the atoms to bond when they are close together, we know their polarization must be antiparallel to each other, let atom a to have an up total spin and atom b to have a down total spin:

$$|POL\rangle = |\uparrow\rangle_a |\downarrow\rangle_b{}^1 \qquad (2.2)$$

The similarity of these wave functions can be calculated with the squared inner product:

$$
\begin{aligned}
\langle POL|UPO\rangle &= \left(\langle\uparrow|_a \langle\downarrow|_b\right)\left(\frac{1}{\sqrt{4}}\left(|\uparrow\rangle_a |\downarrow\rangle_a + |\uparrow\rangle_a |\downarrow\rangle_b + |\uparrow\rangle_b |\downarrow\rangle_a + |\uparrow\rangle_b |\downarrow\rangle_b\right)\right)\\
&= \frac{1}{2}\left(\delta_{a,a}\delta_{b,a} + \delta_{a,a}\delta_{b,b} + \delta_{a,b}\delta_{b,a} + \delta_{a,b}\delta_{b,b}\right)\\
\langle POL|UPO\rangle &= \frac{1}{2}\left(0 + 1 + 0 + 0\right)\\
\langle POL|UPO\rangle &= \frac{1}{2}\\
\langle POL|UPO\rangle^2 &= \frac{1}{4} \qquad (2.3)
\end{aligned}
$$

---

[1]Here, we use the three letter acronyms "UPO" unconventionally to designate the in the infinite bond-length limit, there are a number of states that are degenerate with the ground state, and "POL" to designate that some of these states correspond to mixtures of open shell states.

7

This is an expected result, we can see the $|\uparrow\rangle_a |\downarrow\rangle_b$ state contributes a quarter to the unpolarized wave function.

In general, the unpolarized state is given by:

$$|UPO\rangle = \frac{1}{2^N} \sum_{\theta \epsilon S_{2N}} \prod_j^N |\uparrow\rangle_{\theta(j)} |\downarrow\rangle_{\theta(j)} \qquad (2.4)$$

where N is the number of unpaired electrons of one atom, θ is an array of $2N$ localizations for each electron (either around atom a or b), S_{2N} is the array of all the possible arrays of combinations for θ. From this definition we can easily see that any θ contributes $\frac{1}{2^N}$ to the unpolarized wave function. This means that the probability of finding the specific state $|POL\rangle = \prod_{j=1}^N |\uparrow\rangle_{a_j} |\downarrow\rangle_{b_j}$ is $\frac{1}{2^{2N}}$. In table 2.1 we can review the expected overlaps of polarized and unpolarized wave functions, as well as the related probability for systems with different amounts of unpaired electrons.

Table 2.1: Expected Overlaps and Probabilities
for 2N Unpaired Electron Systems

2N	Overlap	Probability
2	$\frac{1}{\sqrt{4}}$	$\frac{1}{4} = 0.25$
4	$\frac{1}{\sqrt{16}}$	$\frac{1}{16} = 0.0625$
6	$\frac{1}{\sqrt{64}}$	$\frac{1}{64} = 0.015625$
12	$\frac{1}{\sqrt{4096}}$	$\frac{1}{4096} = 0.24414062 \times 10^{-3}$

Very Close Atoms

As two polarized atoms get closer, their electrons start to interact with the other atom, making it impossible to distinguish to which atom they belong to; because we are interested in bonded atoms, and the electrons become indistinguishable, the wave function of two originally polarized atoms that have bonded would be:

$$|\Psi\rangle = |\uparrow\rangle\,|\downarrow\rangle \tag{2.5}$$

There are no atom indices as before because the particles are indistinguishable.

Equation (2.5) matches the wave function of an unpolarized pair of indistinguishable atoms with total spin of zero; meaning that the inner product of these wave functions is equal to one. A very insightful interpretation of this result is that as two polarized atoms get closer to form a dimer, the overall wave function of the systems starts to collapse into that of a pair of unpolarized atoms.

2.2 Coulson Fischer Point

In 1949, Coulson and Fischer published a paper on how to build, from molecular orbital wave functions, an accurate wave function that would take into account the repulsion between electrons as the atoms are separated, and applied it to H_2 obtaining amazing results [18]. Unlike the other methods at the time, Coulson-Fischer theory provided a qualitatively correct description of the molecular dissociation process [19]. It should be noted that, like many good ideas in science, Heitler and London may have been the first to describe a special case for this and that understanding these ideas is important from the standpoint of understanding Mott Insulators in solid state physics [20].

According to Coulson and Fischer, a wave function of the form:

$$|\Psi\rangle = \frac{1}{2}(|\phi_a(r_1)\rangle + |\phi_b(r_1)\rangle) \cdot (|\phi_a(r_2)\rangle + |\phi_b(r_2)\rangle) \cdot SpinTerm \qquad (2.6)$$

where $|\phi_a\rangle, |\phi_b\rangle$ are the real orbitals of an electron around atom a, and atom b, respectively, does not considers the repulsion between electrons as the atoms are separating. Coulson and Fischer proposed that, instead of using equation (2.7), the wave function could have the form:

$$|\Psi\rangle = \frac{1}{1 + \lambda S + \lambda^2}(|\phi_a(r_1)\rangle + \lambda|\phi_b(r_1)\rangle) \cdot (|\phi_b(r_2)\rangle + \lambda|\phi_a(r_2)\rangle) \cdot SpinTerm \qquad (2.7)$$

where λ is a parameter that is not necessarily one, and S is the overlap between orbitals $|\phi_a\rangle$ and $|\phi_b\rangle$. The distance at which electrons start localizing around a nucleus each, that equation (2.7) starts to fail, or that λ is not equal to one is known as the Coulson-Fischer (CF) point, which has been an interesting reference point for the study of dimers and their excited states[21].

2.3 Motivation

Here we must ask ourselves, how close is enough for a dimer's polarized solution to collapse onto a bonded pair of unpolarized atoms? Is DFT going to offer a physically accurate

answer about the similarity of the polarized and unpolarized solutions for pairs of same element atoms as they get closer together?

2.4   Overlap

Unlike witches and ducks, we can't just throw two electron densities into a large scale and compare them, we must do it differently.

As we saw in subsection 1.2.2, DFT can be worked with orbitals that are directly related to the electron density. But how do we arrange our orbitals in order to have an organized way to compare two densities?

2.4.1   Slater Determinant

Because electrons are fermions, their wave function must be anti-symmetric in order to comply with Pauli's exclusion principle. For two electrons, we could have:

$$|\Psi\rangle = |\chi_1(r_a)\rangle \, |\chi_2(r_b)\rangle \tag{2.8}$$

or

$$|\Psi\rangle = |\chi_2(r_a)\rangle \, |\chi_1(r_b)\rangle \tag{2.9}$$

But neither of these wave functions comply with Pauli's exclusion principle, because they are not anti-symmetric.

We can write a linear combination to find a solution that is anti-symmetric:

$$|\Psi\rangle = \frac{1}{\sqrt{2}}\big(|\chi_1(r_a)\rangle \, |\chi_2(r_b)\rangle - |\chi_2(r_a)\rangle \, |\chi_1(r_b)\rangle\big) \tag{2.10}$$

This wave function is anti-symmetric, does not favor any electron to occupy certain orbital, and vanishes if the electrons occupy the same orbital.

This expression can be written in a different form:

$$|\Psi\rangle = \frac{1}{\sqrt{2}} \begin{vmatrix} |\chi_1(r_a)\rangle & |\chi_1(r_b)\rangle \\ |\chi_2(r_a)\rangle & |\chi_2(r_b)\rangle \end{vmatrix} \quad (2.11)$$

Equation (2.11) is known as a Slater determinant for a two particle system. Slater introduced this notation in 1929, in order to ensure the anti-symmetry of many-electron systems [22], but it can be used for any kind of fermions. An N-fermionic system Slater determinant looks like:

$$|\Psi\rangle = \frac{1}{\sqrt{N!}} \begin{vmatrix} |\chi_1(r_a)\rangle & |\chi_1(r_b)\rangle & \cdots & |\chi_1(r_N)\rangle \\ |\chi_2(r_a)\rangle & |\chi_2(r_b)\rangle & \cdots & |\chi_2(r_N)\rangle \\ \vdots & \vdots & \ddots & \vdots \\ |\chi_N(r_a)\rangle & |\chi_N(r_b)\rangle & \cdots & |\chi_N(r_N)\rangle \end{vmatrix} \quad (2.12)$$

Or, in Leibniz notation:

$$|\Psi\rangle = \frac{1}{\sqrt{N!}} \sum_{\sigma \in S_N} \text{Sign}(\sigma) \prod_{j}^{N} |\chi_{\sigma(j)}(r_j)\rangle \quad (2.13)$$

where σ is an array and S_N is an array of all the permutations of $\{1, 2, \cdots, N\}$, and has $N!$ cardinality. For example, for $N = 1, 2, 3$ we would have the following σ's:

Table 2.2: $\sigma(1), \sigma(2), \sigma(3)$

N	1	2	3	Sign(σ)
σ_1	{1}	{1,2}	{1,2,3}	+
σ_2		{2,1}	{1,3,2}	-
σ_3			{3,1,2}	+
σ_4			{3,2,1}	-
σ_5			{2,3,1}	+
σ_6			{2,1,3}	-

Do not confuse σ_i with $\sigma(j)$, the latter refers to the j-th element of the current σ,

while the former is just used for this example as it is unnecessary to use the i index for our notation.

From linear algebra we know that a determinant can be obtained as the summation of the product of cofactors (any element of a matrix, preceded by a $-$ or a $+$, depending on the row and column) and their minor (the submatrix formed by removing the row and column related to its cofactor), over any row or column. From this property of determinants we can obtain a very insightful idea of fermionic systems: the Slater determinant of an N-fermionic system can be broken down into N Slater determinants of order N-1, if the N-fermionic Slater determinant is non zero, there must be at least one non-zero minor as well [23].

2.4.2 Inner Product of Slater Determinants

Before we look for the expression to calculate the inner product, or overlap, of two different Slater determinants, we must show that equation (2.13) is correctly normalized.

Same Slater Determinant

$$\langle \Psi | \Psi \rangle = \frac{1}{\sqrt{N!}} \sum_{\lambda \epsilon S_N} \text{Sign}(\lambda) \prod_j^N \langle \chi_{\lambda(j)}(r_j)| \frac{1}{\sqrt{N!}} \sum_{\sigma \epsilon S_N} \text{Sign}(\sigma) \prod_k^N |\chi_{\sigma(k)}(r_k)\rangle$$

$$= \frac{1}{N!} \sum_{\lambda,\sigma \epsilon S_N} \text{Sign}(\lambda)\text{Sign}(\sigma) \prod_{j,k}^N \langle \chi_{\lambda(j)}(r_j)|\chi_{\sigma(k)}(r_k)\rangle$$

Here we must point out that bras and kets permute until they are matched with the correct particle. This means that having to products, one for k and j, has no sense, as we only need one.

$$\langle \Psi | \Psi \rangle = \frac{1}{N!} \sum_{\lambda,\sigma \epsilon S_N} \text{Sign}(\lambda)\text{Sign}(\sigma) \prod_j^N \langle \chi_{\lambda(j)}(r_j)|\chi_{\sigma(j)}(r_j)\rangle$$

If the set $\{|\chi_i\rangle\}$ is an orthonormal set, then:

$$\langle \chi_{\lambda(j)}|\chi_{\sigma(j)}(r_k)\rangle = \delta_{\lambda(j),\sigma(j)}$$

$$\rightarrow \prod_j^N \langle \chi_{\lambda(j)}(r_j)|\chi_{\sigma(j)}(r_j)\rangle = \delta_{\lambda,\sigma \epsilon S_N}$$

$$\rightarrow \sum_{\lambda,\sigma \epsilon S_N} \text{Sign}(\lambda)\text{Sign}(\sigma)\delta_{\lambda,\sigma} = \sum_{\lambda \epsilon S_N} 1 = N!$$

$$\langle \Psi|\Psi\rangle = 1 \tag{2.14}$$

Different Slater Determinant

Before we get to the general case, lets for a second consider a two particle problem to give us some insight:

$$\langle \Phi|\Psi\rangle = \frac{1}{2}\big(\langle \xi_1(r_1)|\chi_1(r_1)\rangle \langle \xi_2(r_2)|\chi_2(r_2)\rangle - \langle \xi_2(r_1)|\chi_1(r_1)\rangle \langle \xi_1(r_2)|\chi_2(r_2)\rangle$$
$$- \langle \xi_1(r_1)|\chi_2(r_1)\rangle \langle \xi_2(r_2)|\chi_1(r_2)\rangle + \langle \xi_2(r_1)|\chi_2(r_1)\rangle \langle \xi_1(r_2)|\chi_1(r_2)\rangle \big)$$

as we know, a braket represents an integral, which means that two brakets with the same orbitals have the exact same value regarding the particle they are associated.

$$\rightarrow \langle \Phi|\Psi\rangle = \frac{1}{2}\big(\langle \xi_1|\chi_1\rangle \langle \xi_2|\chi_2\rangle - \langle \xi_2|\chi_1\rangle \langle \xi_1|\chi_2\rangle$$
$$- \langle \xi_1|\chi_2\rangle \langle \xi_2|\chi_1\rangle + \langle \xi_2|\chi_2\rangle \langle \xi_1|\chi_1\rangle \big)$$
$$= \frac{1}{2}\big(2\langle \xi_1|\chi_1\rangle \langle \xi_2|\chi_2\rangle - 2\langle \xi_1|\chi_2\rangle \langle \xi_2|\chi_1\rangle \big)$$
$$= \langle \xi_1|\chi_1\rangle \langle \xi_2|\chi_2\rangle - \langle \xi_1|\chi_2\rangle \langle \xi_2|\chi_1\rangle$$

$$\tag{2.15}$$

As we can notice this has a shape that we know.

$$\langle \Phi|\Psi\rangle = \begin{vmatrix} \langle \xi_1|\chi_1\rangle & \langle \xi_1|\chi_2\rangle \\ \langle \xi_2|\chi_1\rangle & \langle \xi_2|\chi_2\rangle \end{vmatrix} \tag{2.16}$$

14

This is no proof that in general we would have a determinant, but it gives us a hint of what to look for.

Now we can go to the general two Slater determinant product.

$$\langle\Phi|\Psi\rangle = \frac{1}{\sqrt{N!}}\sum_{\lambda\epsilon S_N}\text{Sign}(\lambda)\prod_j^N \langle\xi_{\lambda(j)}(r_j)|\frac{1}{\sqrt{N!}}\sum_{\sigma\epsilon S_N}\text{Sign}(\sigma)\prod_k^N|\chi_{\sigma(k)}(r_k)\rangle$$

$$= \frac{1}{N!}\sum_{\lambda,\sigma\epsilon S_N}\text{Sign}(\lambda)\text{Sign}(\sigma)\prod_{j,k}^N \langle\xi_{\lambda(j)}(r_j)|\chi_{\sigma(k)}(r_k)\rangle$$

Once again, as we know bras and kets permute until they are matched with the correct particle, so we can drop a product.

$$\langle\Phi|\Psi\rangle = \frac{1}{N!}\sum_{\lambda,\sigma\epsilon S_N}\text{Sign}(\lambda)\text{Sign}(\sigma)\prod_j^N \langle\xi_{\lambda(j)}(r_j)|\chi_{\sigma(j)}(r_j)\rangle$$

Notice that, because brakets don't really care for the coordinate the orbital is dependent on, i.e. r_j, we can drop that from our expression.

$$\langle\Phi|\Psi\rangle = \frac{1}{N!}\sum_{\lambda,\sigma\epsilon S_N}\text{Sign}(\lambda)\text{Sign}(\sigma)\prod_j^N \langle\xi_{\lambda(j)}|\chi_{\sigma(j)}\rangle$$

For any λ, σ pair, we can permute brackets until we recover what would appear to be an arbitrary λ. As an example, consider we want to permute brakets in order to have our bra's with the orbitals ordered as their labels, i.e. $\lambda = \{1, 2, \cdots, N\}$, which always has a positive permutation Sign, $\text{Sign}(\lambda) = +$, for N=3:

Table 2.3: Permutations for $\lambda = \{3, 2, 1\}$

λ	σ's	$\text{Sign}(\lambda)\text{Sign}(\sigma)$	σ'	$\text{Sign}(\sigma')$
$\{3,2,1\}$	$\{1,2,3\}$	-	$\{3,2,1\}$	-
	$\{1,3,2\}$	+	$\{2,3,1\}$	+
	$\{3,1,2\}$	-	$\{2,1,3\}$	-
	$\{3,2,1\}$	+	$\{1,2,3\}$	+
	$\{2,3,1\}$	-	$\{1,3,2\}$	-
	$\{2,1,3\}$	+	$\{3,1,2\}$	+

this means that for every time we sum over σ for any λ, we recover the same components with the same Sign as for the original, and arbitrary, $\lambda' = \{1, 2, \cdots, N\}$:

$$\rightarrow \sum_{\lambda, \sigma \epsilon S_N} \text{Sign}(\lambda)\text{Sign}(\sigma) \prod_j^N \langle \xi_{\lambda(j)} | \chi_{\sigma(j)} \rangle = N! \sum_{\sigma \epsilon S_N} \text{Sign}(\sigma) \prod_j^N \langle \xi_j | \chi_{\sigma(j)} \rangle$$

$$\rightarrow \langle \Phi | \Psi \rangle = \sum_{\sigma \epsilon S_N} \text{Sign}(\sigma) \prod_j^N \langle \xi_j | \chi_{\sigma(j)} \rangle \qquad (2.17)$$

Equation (2.17) is Leibniz notation for a determinant. If we compare it with equation (2.13), the (r_j) would be replaced with the $\langle \xi_j |$ as the naturally ordered component, while the $| \chi_{\sigma(j)} \rangle$ is the array dependent component just as before.

This result indicates that, in order to compare two electron densities, we can build a matrix with the overlap of the Kohn-Sham orbitals of each density, and calculate the determinant of this overlap matrix.

$$\langle \Phi | \Psi \rangle = \begin{vmatrix} \langle \xi_1 | \chi_1 \rangle & \langle \xi_1 | \chi_2 \rangle & \cdots & \langle \xi_1 | \chi_N \rangle \\ \langle \xi_2 | \chi_1 \rangle & \langle \xi_2 | \chi_2 \rangle & \cdots & \langle \xi_2 | \chi_N \rangle \\ \vdots & \vdots & \ddots & \vdots \\ \langle \xi_N | \chi_1 \rangle & \langle \xi_N | \chi_2 \rangle & \cdots & \langle \xi_N | \chi_N \rangle \end{vmatrix} \qquad (2.18)$$

This result has been used before by Michalak, and peers [24].

16

Chapter 3

Methodology

3.1   NRLMOL

The computational tool used to perform DFT calculations presented in this work is the Naval Research Laboratory Molecular Orbital Library (NRLMOL)[25, 26]. NRLMOL is a massively parallel DFT code based on the Kohn-Sham formulation, which solves the Kohn-Sham equations by expressing the KS orbitals as linear combinations of Gaussian orbitals [27].

The exchange correlation potential used was PBE-GGA (Perdew–Burke-Ernzerhof, General Gradient Approximation). The overlap tool has been developed to be used on Kohn-Sham orbitals obtained from any potential, and we will not worry about the differences that could be shown from using different potentials in this work. The electronic energy optimization were done with a convergence criteria of $0.100x10^{-7}$ Ha.

The overlap of the Slater determinants has been calculated using the methodology described in 2.4.2. The computational tool that performs this task has been implemented into NRLMOL, along with other features in order to automatize pre-processing needs, such as gathering and renaming of WFOUT files, building directories and writing files with information regarding the overlap calculation.

3.2   Dimer Calculations

In order to compare the Slater determinants of polarized and unpolarized atoms, NRL-MOL allows us to pick the kind of polarization we are interested in, either up, down or

unpolarized.

As we intended to study the collapse of a polarized system into a bonded pair of unpolarized atoms, we performed two sets of calculations, following a series of steps, editing some of the input files of NRLMOL:

1. Start a calculation with two atoms of the same element.

2. Edit the SYMBOL file to include more calculations, bringing the atoms together.

3. Edit the first line of the SYMBOL file to SCF-ONLY.

4. Edit the RUNS file to start our first calculation using a Least Square Fit.

5. Save the wave function file (WFOUT) with an appropriate name to remember to which calculation it is associated.

6. Repeat until all calculations are done.

7. On the SYMBOL file, substitute the first UPO flag of each calculation for SUP and the second one for SDN.

8. Repeat from step 4 to 7.

The energies of each calculation can be reviewed on the ALL-FORCES file.

3.3   Overlap Calculations

Once we had our wave function files from each calculation, finding the overlap between two of these files is fairly easy:

1. Edit the MODE file to the overlap mode (3).

2. Save all wavefunction files on a new directory.

3. Edit the RUNS file to start from the first calculation.

4. Copy the pair of wave function files associated with the first calculation to the current directory.

5. Run the calculation, the overlap can be found on the overlap file.

6. Edit the RUNS file to do the following calculation.

7. Delete all the wave function files in the current directory.

8. Copy the pair of wavefunction files associated with the following calculation to the current directory.

9. Repeat from step 5 to 8.

3.4   Hysteresis Calculations

An interesting test that can be performed to show how the polarized wave function collapses into an unpolarized is to bring together the two polarized atoms, once they pass through the CF point, we start separating them again and show that the energy is now the one of an unpolarized pair of atoms, this is similar to the magnetic hysteresis phenomena, but instead of having a physical defect we have the collapse of the wave function. To do this test we follow the next steps:

1. Start a calculation with two atoms of the same element, one must have an SUP flag and the other an SDN one separated far away.

2. Edit the SYMBOL file to include more calculations, bringing the atoms together beyond the CF point.

3. Include calculations separating the atoms, these must have UPO flags (this does not force the atoms to be unpolarized but takes out the restriction of polarization if they are far enough).

4. Edit the first line of the SYMBOL file to SCF-ONLY.

5. Edit the RUNS file to start our first calculation using a Least Square Fit.

6. Repeat until all calculations are done.

7. Repeat all steps, but in step 3, instead of going beyond the CF point, start separating the atoms before the CF point is reached.

You can find the SYMBOL, ISYMGEN and runit files to do either the energies or the hysteresis calculations for Cr_2 on my github:
"https://github.com/JGustavoBFlores/Cr2_Dimer_Input_Files"[1]. According to which calculation you want to do, rename the respective SYMBOL file to SYMBOL, these would work with any NRLMOL version. For the overlap calculation, contact me through github to receive a copy of the overlap code.

These calculations will show two different curves: both will be along the polarized curve up to the CF point, if the CF point is reached, we should see the energy curve go back along the unpolarized energy curve, if the CF point is never reached, the energy curve should go back along the polarized curve again.

---

[1]If the repository is unavailable, contact me through github.

Chapter 4

Results

4.1 H$_2$

The H$_2$ dimer, although being a simple and the smallest dimer in nature, still draws the attention of many researchers from different areas, from chemists to astrophysicists, who basically do far far away spectroscopy or past spectroscopy if you are a relativity fan [28]. An important remark of the importance of H$_2$ lies in how the decomposition of H$_2$ to atomic H is related to the loss of water in any planet, studies have been done about Mars for example [29, 20].
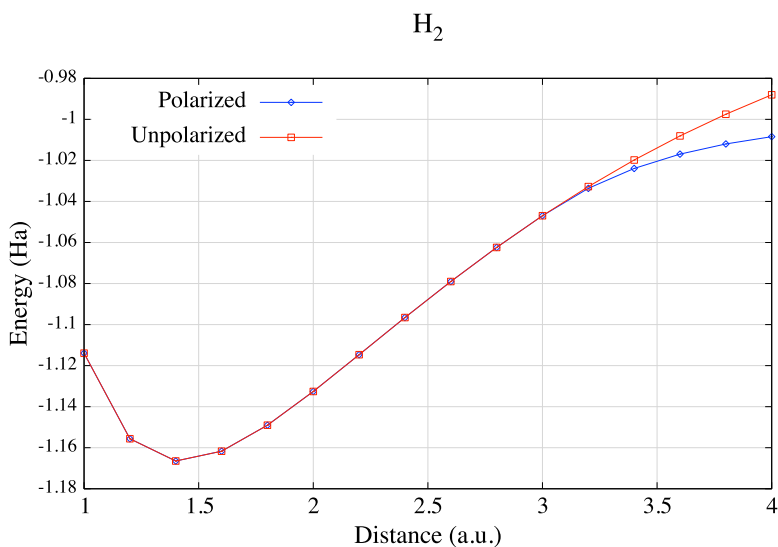

Figure 4.1: H$_2$ Potential Curves

As we can see from figure 4.1, the energy curves of the polarized and unpolarized states match together from very far away, compared with the bond distance of 1.42 a.u. The

energies match up at 3.0. a.u., which for our further analysis will be referred to as the CF point for H_2. At 3.2 a.u. the energies difference is $0.85x10^{-3}$ Ha, relatively big for our convergence criteria, this indicates that our Slater determinants must be different, but how much?
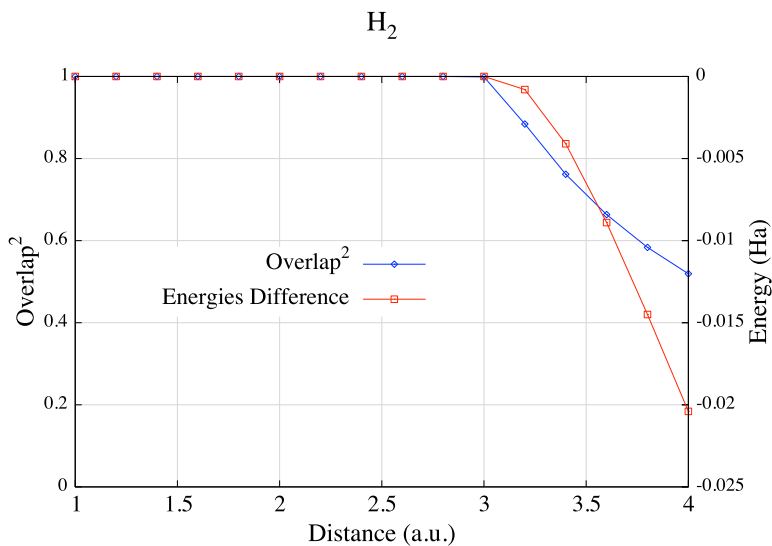

Figure 4.2: H_2 Overlap and Energy Difference

On figure 4.2 we have two curves to compare how the difference between the polarized and unpolarized energies, and the overlap or similitude of Slater determinants relate to each other. As we can see, as long as the energies difference is zero, the overlap remains as one. Once the energy difference is non zero, as we can see starting at 3.2 a.u., the Slater determinants start to differ. For 3.2 a.u. we have an overlap of 0.8841. The overlap of calculations beyond 4.00 a.u. are shown in the following figure:
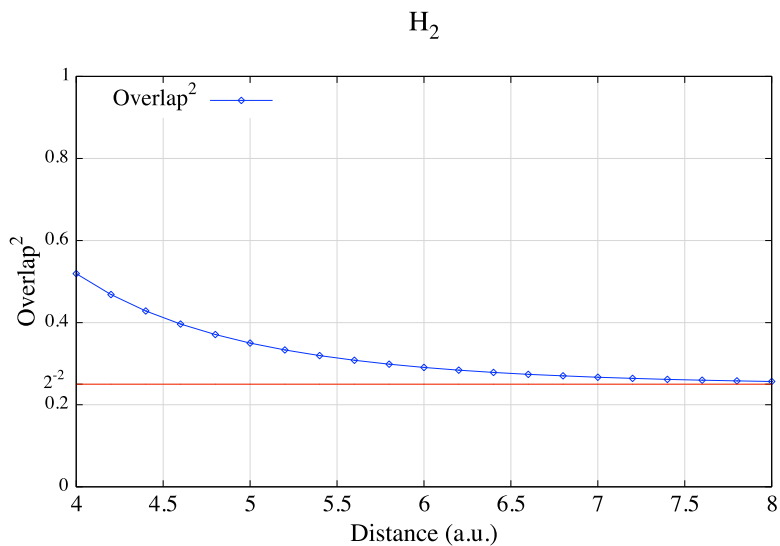
Figure 4.3: H_2 Overlaps beyond 4.0 a.u.

Because H has a single electron, the behaviour of the overlap between unpolarized and polarized states at an infinite separation can be explained by using subsection 2.1.1 description. We can extrapolate from the data shown on figure 4.3, that at an infinite distance, the overlap matches $\frac{1}{4}$, as predicted in subsection 2.1.1.
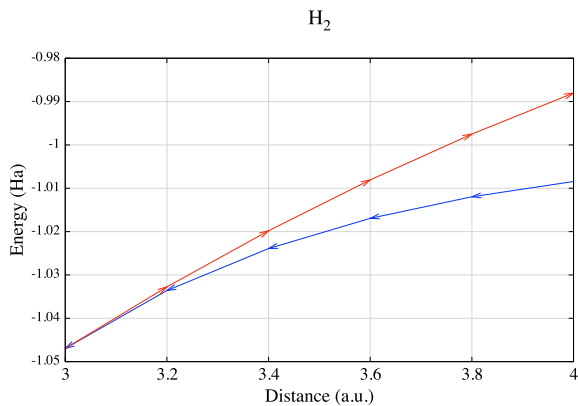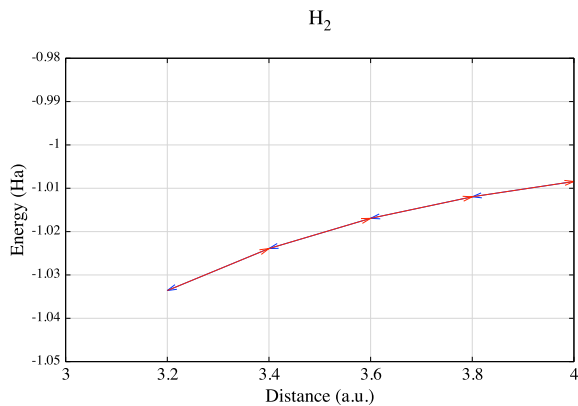

Figure 4.4: H_2 Beyond the CF Point

Figure 4.5: H_2 Before the CF Point

In figure 4.4 we show how, after bringing the atoms closer (blue trajectory) than the CF point, our polarized Slater determinant in fact turns into the unpolarized one, and by

23

separating (red trajectory) the atoms, we do not recover the polarized energies but the unpolarized ones. Figure 4.5 shows how if we start separating (red trajectory) the atoms before reaching the CF point, the energy follows the same curve in the opposite direction on each site, remaining in the polarized curve. This analysis shows us how the collapse of the polarized Slater determinant into the unpolarized one could not occur at 3.2 a.u., it must happen with a larger overlap than 0.8841, at least for this system.

4.2   N$_2$

Nitrogen is perhaps one of the most important elements in the modern world, from medical applications to electronics and fertilizers, the interest on Nitrogen is not constrained to its atomic presentation, but the dimer and the family of nitrogen oxides (NO$_x$) [30], besides the many applications, Nitrogen is also of interest to the environmental scientists because of its relation with the green house effect, as human activities have affected the natural cycle of Nitrogen [31]. Nitrogen's electronic configuration is 1s^{2}2s^{2}2p^3, the three electrons on the 2p orbital energy level are unpaired.
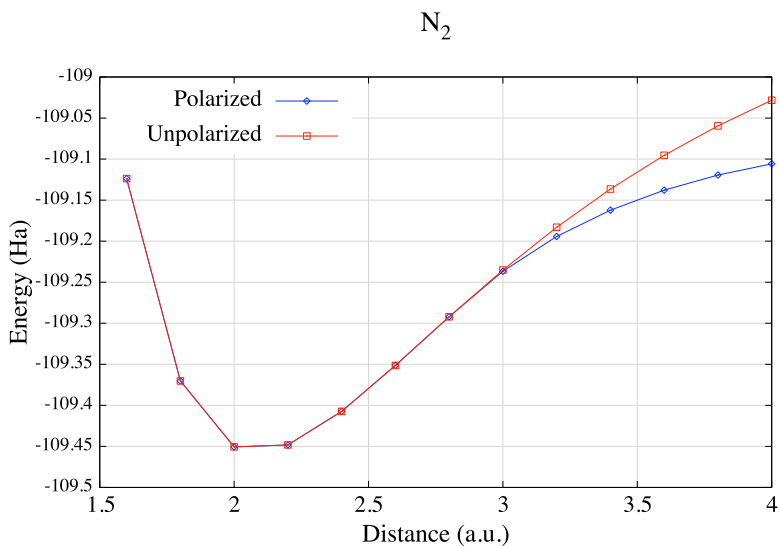

Figure 4.6: N$_2$ Potential Curves

N$_2$ energy curves hold the same shape as H$_2$, the polarized solution collapsed into the unpolarized solution at about twice of the bond distance. The energies exactly match at 2.8 a.u., while at 3.0 a.u. the difference is of $0.14x10^{-2}$ Ha, which is big for our convergence criteria, as it happened in H$_2$.
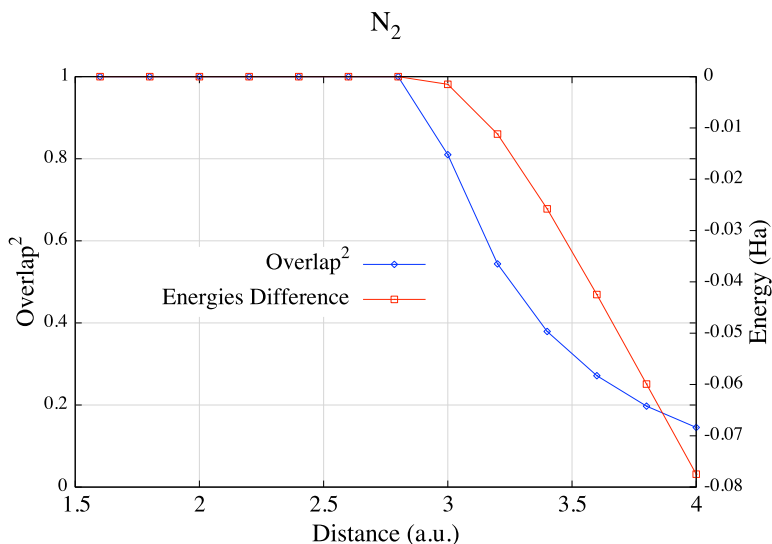

Figure 4.7: N$_2$ Overlap and Energy Difference

As we can see from figure 4.7, at 2.8 a.u. we do have a perfect match in the overlap and the energies, meaning our polarized Slater determinant completely collapsed into the unpolarized one, we can confirm this with figure 4.9, whose analysis is ahead. At 3.0 a.u., we find an overlap of 0.8097, considering our results from H$_2$, this overlap should not be enough for the collapse of the polarized Slater determinant into the unpolarized one to happen.
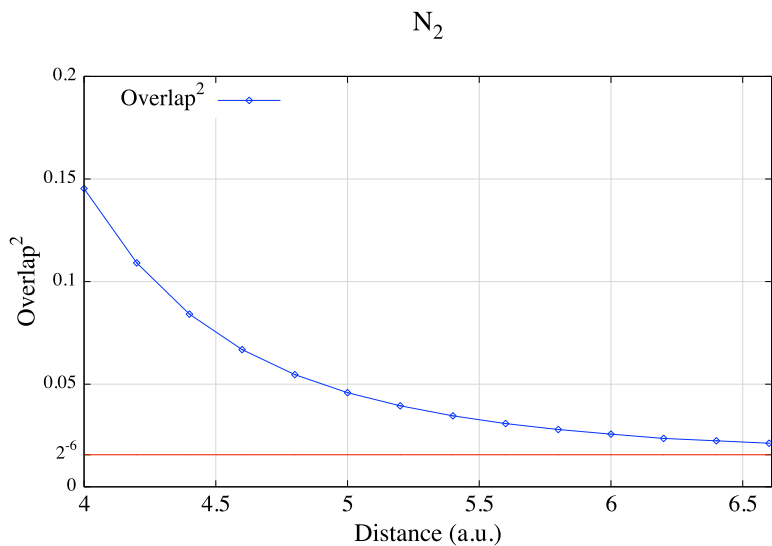
Figure 4.8: N_2 Overlaps beyond 4.0 a.u.

Because N has a three unpaired electrons, the behaviour of the overlap between unpolarized and polarized states at an infinite separation, according to subsection 2.1.1 $\frac{1}{2^3} = 0.125$. We can extrapolate from the data shown on figure 4.8, that at an infinite distance, the overlap matches $\frac{1}{2^6}$, as predicted in table 2.1. Because single atoms of Nitrogen are naturally polarized, separating two bonded Nitrogen atoms, while fixing the magnetic moment to zero, so that each atom remains unpolarized is not an easy task.
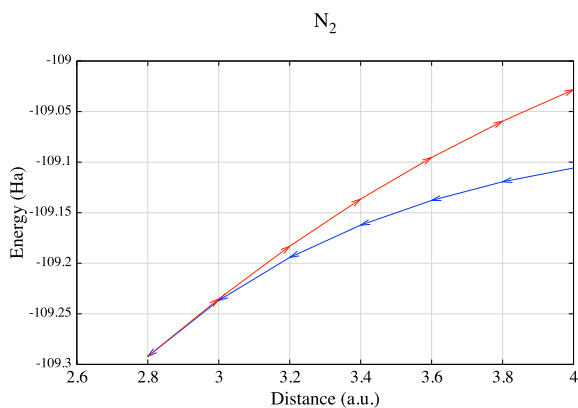

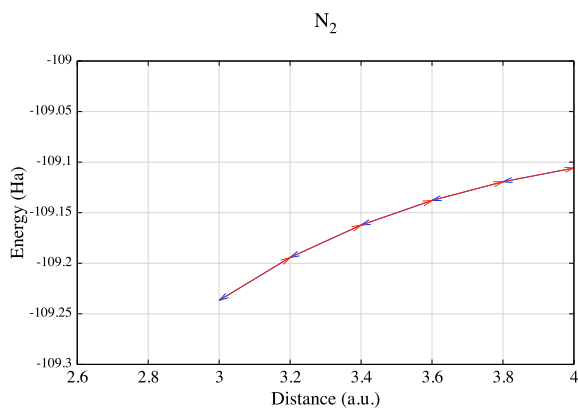Figure 4.9: N_2 Beyond the CF Point

Figure 4.10: N_2 Before the CF Point

In figures 4.9 and 4.10 we have the have repeated the hysteresis test for the Nitrogen dimer. As it happened with H_2, Figure 4.10 points out that our polarized solution does not decay into the unpolarized at 3.0 a.u., as mentioned in the overlap analysis, the collapse must happen in some point in between 2.8 and 3.0 a.u.

4.3 Cr_2

Chromium dimer has been subject of interest of many chemists and physicists, because of its peculiar electronic structure, magnetic properties, and potential energy curve [32].

The electronic configuration of Chromium is $1s^2 2s^2 2p^6 3s^2 3p^6 3d^5 4s^1$, with twenty four electrons, where six of these are unpaired, these electrons spins always point in the same direction on an isolated atom, which gives Chromium its magnetic properties. It is important to notice that the 3d orbital can hold five electrons per spin, but Chromium has only five electrons on the 3d orbital, and a single electron in the 4s orbital, because this is a more stable configuration than having a pair of paired electrons and four unpaired electrons on the 3d orbital. The bond of two Chromium atoms depends on the spin orientation of these unpaired atoms, as we saw on chapter 2.
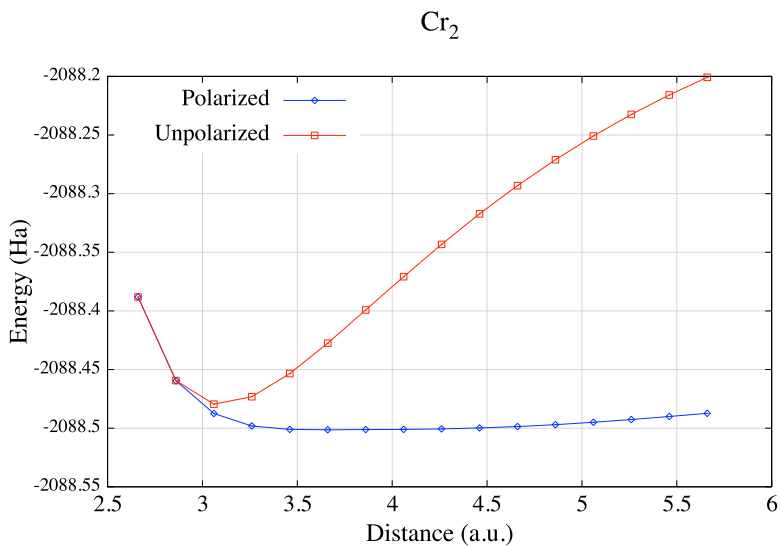
Figure 4.11: Cr_2 Potential Curves

As we can see from figure 4.11, the polarized state is, generally, more stable than the unpolarized one. As we mentioned before, single Chromium atoms tend to be polarized, forcing an unpolarized solution for this system at a large separation goes against Chromium's nature, that is why the unpolarized energy curve differs so much from the polarized one, and it is very difficult to achieve convergence for an unpolarized calculation at these separations. Our energy curves match around 2.8 a.u., and the obtained bond distance is around 3.17 a.u., which coincides with the experimentally reported [33]. A very interesting fact to take from this figure is that, even at the most stable point for Cr_2, the polarized and unpolarized have different energies, which indicates they have different Slater determinants.
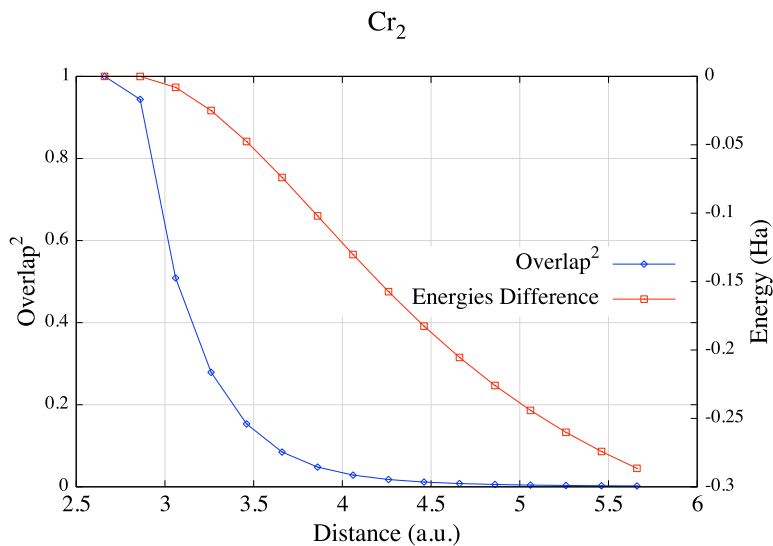
Figure 4.12: Cr_2 Overlap and Energies Difference

As predicted in the analysis of figure 4.11, the Slater determinants of both calculations are different at 3.06 a.u., with an overlap of 0.5088. At 2.86 a.u. we find matching energies, but an overlap of 0.9441, which indicates our polarized solution has not collapsed into the unpolarized solution completely. Will this overlap be enough for the polarized Slater determinant to swap from the polarized energy curve into the unpolarized one?
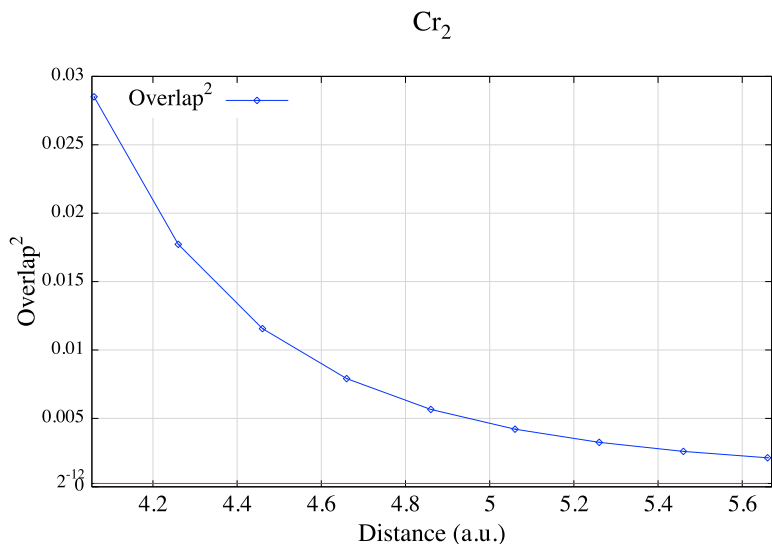
Figure 4.13: Cr_2 Overlaps beyond 4.0 a.u.

As Nitrogen, Chromium has more than one unpaired electron, it has six unpaired electrons, this means that the overlap squared between unpolarized and polarized states at an infinite separation, is $\frac{1}{2^{12}} = 0.244 \times 10^{-3}$. Because single atoms of Chromium are naturally polarized, separating two bonded Chromium atoms, while fixing the magnetic moment so that each atom remains unpolarized is an even harder task than for Nitrogen.
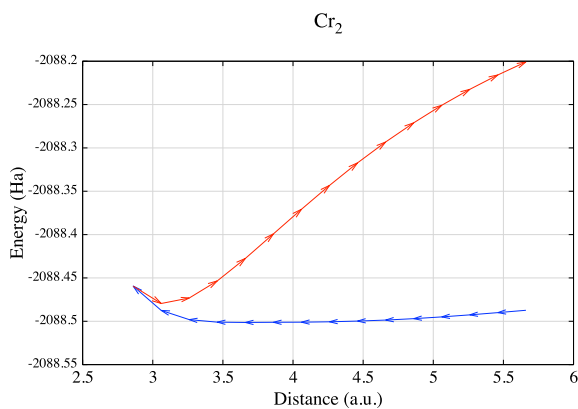

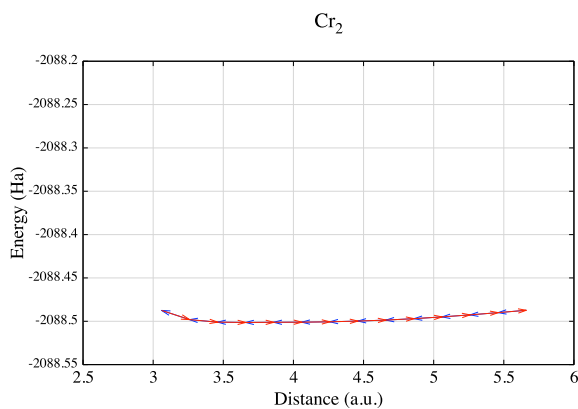Figure 4.14: Cr_2 Beyond the CF Point

Figure 4.15: Cr_2 Before the CF Point

We conclude from figure 4.14, that the overlap of 0.9441 is enough for the collapse to

happen. This indicates that it is not mandatory for the polarized solution to completely converge into the unpolarized state for a switch of energy curves to happen. From figure 4.15, we can conclude that having two Chromium atoms with different polarizations at 3.06 a.u., which is closer than the experimentally reported bond distance [33], is not sufficient for a bond to be formed. We could deduce that there must exist a point where this also happens for H_2 and N_2, with the caveat this result is no proof of a general behaviour of dimer's Slater determinants.

4.4 Dimer's Bond Lengths

In table 4.1, we show the bond lengths , using the same converge criteria as on our past calculations, as well as other computational and experimental data to compare with.

Table 4.1: Dimers Bond Lengths

Dimer	Our Results (a.u.)	Computational (a.u.)	Experimental (a.u.)
H2	1.42	1.401 (ref: [34])	1.400 (ref: [35])
N2	2.085	2.475 (ref: [36])	2.074 (ref: [37])
Cr2	3.091	3.250 (ref: [38])	3.174 (ref: [39])

As we can see, our calculations are in very good agreement with the experimental results. Our H_2, N_2, and Cr_2 calculations have percent errors of 1.42%, 0.53%, 2.61%, respectively.

Chapter 5

Concluding Remarks

5.1 Significance of Our Results

As we have seen in our three different systems, finding the Coulson-Fischer point is not a task to rely on one method. There are cases where, although the energies of polarized and unpolarized states are very close or even equal, their Slater determinants are different and there is not decay into the unpolarized solution. Empirically, we could point out that the overlap squared of Slater determinants for polarized and unpolarized solutions of a dimer seems to follow the shape of the error function, converging to $\frac{1}{2^N}$, where N is the number of unpaired electrons per atom from the dimer, as we have seen in our three examples. We have shown that there is a relation between the energy differences and the overlap of unpolarized and polarized Slater determinants. The collapse of a polarized Slater determinant into an unpolarized one does not require a perfect overlap. Studying the overlap of polarized and unpolarized states for a dimer at large separations becomes a harder task if there are more than one unpaired electrons per atom.

5.2 Applications and Future Work

The overlap tool that was developed for this work has served for research of other systems, such as ozone (O_3), for which the overlap machinery was used in order to calculate the overlap matrix between two different magnetic states. Another system that has been worked on is the decay of OH^- with H_3O^+ into $2\,H_2O$, in hopes to find a relation between the overlap of these systems and the pH of water. Introducing symmetry into the overlap

machinery, as well as as a parallel version should be among the next steps for the project. The overlap tool will also be implemented into the FLOSIC methodology [40].

Chapter 6

Related Projects

Along with the work presented here, Gustavo Bravo was involved in other research projects:

1. G. Bravo coauthored the paper "Downward quantum learning from element 118: Automated generation of Fermi–Löwdin orbitals for all atoms" [23]. In this paper, a new algorithm to automate the construction of initial points and orbitals for all elements of the periodic table, starting from the largest 118 element Oganesson Og is proposed. Once the orbitals for Og are found, initial points and orbitals for the 117 element can be proposed, and so on for all elements of the periodic table. G. Bravo's contributions to this project were related to the software development.

2. As mentioned in 5.2, G. Bravo's overlap tool was used in a research project on the ozone molecule. In this project, the two antiferromagnetic states $(|AF_{\uparrow\downarrow}\rangle, |AF_{\downarrow\uparrow}\rangle)$ and the pure singlet state $(|00\rangle)$ are compared using the overlap machinery. Contrary to what is usually supposed, it was obtained that $\langle AF_{\uparrow\downarrow}|00\rangle = \langle AF_{\downarrow\uparrow}|00\rangle \neq 0$ and $\langle AF_{\uparrow\downarrow}|AF_{\downarrow\uparrow}\rangle \neq 0$.[1]

---

[1]This project's results have not been published as of the publication of this thesis.

References

[1] L. de la Peña, *Introducción a la mecánica cuántica.* Ediciones Científicas Universitarias, Fondo de Cultura Economica, 2014.

[2] G. Kirchhoff, "I. On the relation between the radiating and absorbing powers of different bodies for light and heat," *The London, Edinburgh, and Dublin Philosophical Magazine and Journal of Science*, vol. 20, no. 130, pp. 1–21, 1860.

[3] W. Wien, "XXX. On the division of energy in the emission-spectrum of a black body," *The London, Edinburgh, and Dublin Philosophical Magazine and Journal of Science*, vol. 43, no. 262, pp. 214–220, 1896.

[4] F. Lord Rayleigh, "LIII. remarks upon the law of complete radiation," *The London, Edinburgh, and Dublin Philosophical Magazine and Journal of Science*, vol. 49, no. 301, pp. 539–540, 1900.

[5] M. Planck, "Ueber irreversible strahlungsvorgänge," *Annalen der Physik*, vol. 306, no. 1, pp. 69–122, 1900.

[6] A. Einstein, "Über einen die erzeugung und verwandlung des lichtes betreffenden heuristischen gesichtspunkt," *Annalen der Physik*, vol. 322, no. 6, pp. 132–148, 1905.

[7] A. H. Compton, "A quantum theory of the scattering of x-rays by light elements," *Phys. Rev.*, vol. 21, pp. 483–502, May 1923.

[8] L. de Broglie, *Recherches sur la théorie des Quanta.* Theses, Migration - université en cours d'affectation, Nov. 1924.

[9] C. Davisson and L. H. Germer, "Diffraction of electrons by a crystal of nickel," *Phys. Rev.*, vol. 30, pp. 705–740, Dec 1927.

[10] E. Schrödinger, "Quantisierung als eigenwertproblem," *Annalen der Physik*, vol. 384, no. 4, pp. 361–376, 1926.

[11] M. Born and R. Oppenheimer, "Zur quantentheorie der molekeln," *Annalen der Physik*, vol. 389, no. 20, pp. 457–484, 1927.

[12] P. Hohenberg and W. Kohn, "Inhomogeneous electron gas," *Phys. Rev.*, vol. 136, pp. B864–B871, Nov 1964.

[13] W. Kohn and L. J. Sham, "Self-consistent equations including exchange and correlation effects," *Phys. Rev.*, vol. 140, pp. A1133–A1138, Nov 1965.

[14] N. Mardirossian and M. Head-Gordon, "Thirty years of density functional theory in computational chemistry: an overview and extensive assessment of 200 density functionals," *Molecular Physics*, vol. 115, no. 19, pp. 2315–2372, 2017.

[15] T. Q. Teodoro, R. L. A. Haiduke, U. Dammalapati, S. Knoop, and L. Visscher, "The ground-state potential energy curve of the radium dimer from relativistic coupled cluster calculations," *The Journal of Chemical Physics*, vol. 143, no. 8, p. 084307, 2015.

[16] M. Musiał and S. A. Kucharski, "First principle calculations of the potential energy curves for electronic states of the lithium dimer," *Journal of Chemical Theory and Computation*, vol. 10, no. 3, pp. 1200–1211, 2014. PMID: 26580190.

[17] E. Pahl, D. Figgen, C. Thierfelder, K. A. Peterson, F. Calvo, and P. Schwerdtfeger, "A highly accurate potential energy curve for the mercury dimer," *The Journal of Chemical Physics*, vol. 132, no. 11, p. 114301, 2010.

[18] P. C. Coulson and M. I. Fischer, "XXXIV. notes on the molecular orbital treatment of the hydrogen molecule," *The London, Edinburgh, and Dublin Philosophical Magazine and Journal of Science*, vol. 40, no. 303, pp. 386–393, 1949.

[19] V. Glushkov and S. Wilson, "The coulson–fischer wave function: parametrisation using distributed gaussian basis sets," *Molecular Physics*, vol. 107, no. 21, pp. 2299–2308, 2009.

[20] W. Heitler and F. London, "Wechselwirkung neutraler Atome und homöopolare Bindung nach der Quantenmechanik," *Zeitschrift fur Physik*, vol. 44, pp. 455–472, June 1927.

[21] D. Hait, A. Rettig, and M. Head-Gordon, "Beyond the coulson–fischer point: characterizing single excitation ci and tddft for excited states in single bond dissociations," *Physical Chemistry Chemical Physics*, vol. 21, no. 39, pp. 21761–21775, 2019.

[22] J. C. Slater, "The theory of complex spectra," *Phys. Rev.*, vol. 34, pp. 1293–1322, Nov 1929.

[23] M. R. Pederson, A. I. Johnson, K. P. K. Withanage, S. Dolma, G. B. Flores, Z. Hooshmand, K. Khandal, P. O. Lasode, T. Baruah, and K. A. Jackson, "Downward quantum learning from element 118: Automated generation of Fermi–Löwdin orbitals for all atoms," *The Journal of Chemical Physics*, vol. 158, 02 2023. 084101.

[24] L. Michalak, C. M. Canali, M. R. Pederson, M. Paulsson, and V. G. Benza, "Theory of tunneling spectroscopy in a mn_{12} single-electron transistor by density-functional theory methods," *Phys. Rev. Lett.*, vol. 104, p. 017202, Jan 2010.

[25] K. Jackson and M. R. Pederson, "Accurate forces in a local-orbital approach to the local-density approximation," *Phys. Rev. B*, vol. 42, pp. 3276–3281, Aug 1990.

[26] M. R. Pederson and K. A. Jackson, "Variational mesh for quantum-mechanical simulations," *Phys. Rev. B*, vol. 41, pp. 7453–7461, Apr 1990.

[27] D. Porezag and M. R. Pederson, "Optimization of gaussian basis sets for density-functional calculations," *Phys. Rev. A*, vol. 60, pp. 2840–2847, Oct 1999.

[28] L. N. Fletcher, M. Gustafsson, and G. S. Orton, "Hydrogen dimers in giant-planet infrared spectra," *The Astrophysical Journal Supplement Series*, vol. 235, p. 24, mar 2018.

[29] V. A. Krasnopolsky and P. D. Feldman, "Detection of molecular hydrogen in the atmosphere of mars," *Science*, vol. 294, no. 5548, pp. 1914–1917, 2001.

[30] L. Mitáš and R. M. Martin, "Quantum monte carlo of nitrogen: atom, dimer, atomic, and molecular solids," *Physical review letters*, vol. 72, no. 15, p. 2438, 1994.

[31] M. Zaman, M. L. Nguyen, M. Šimek, S. Nawaz, M. J. Khan, M. N. Babar, and S. Zaman, *Emissions of nitrous oxide (N2O) and di-nitrogen (N2) from the agricultural landscapes, sources, sinks, and factors affecting N2O and N2 ratios*. IntechOpen Rijeka, Croatia, 2012.

[32] H. R. Larsson, H. Zhai, C. J. Umrigar, and G. K.-L. Chan, "The chromium dimer: Closing a chapter of quantum chemistry," *Journal of the American Chemical Society*, vol. 144, no. 35, pp. 15932–15937, 2022. PMID: 36001866.

[33] V. Bondybey and J. English, "Electronic structure and vibrational frequency of cr2," *Chemical Physics Letters*, vol. 94, no. 5, pp. 443–447, 1983.

[34] W. Kolos and L. Wolniewicz, "Improved Theoretical Ground-State Energy of the Hydrogen Molecule," *The Journal of Chemical Physics*, vol. 49, pp. 404–410, 09 2003.

[35] G. Herzberg and A. Monfils, "The dissociation energies of the h2, hd, and d2 molecules," *Journal of Molecular Spectroscopy*, vol. 5, no. 1, pp. 482–498, 1961.

[36] E. Baerends, D. Ellis, and P. Ros, "Self-consistent molecular hartree—fock—slater calculations i. the computational procedure," *Chemical Physics*, vol. 2, no. 1, pp. 41–51, 1973.

[37] J. M. Robertson, "Bond character and interatomic distance," *Journal of the Chemical Society (Resumed)*, pp. 131–138, 1938.

[38] H. Dachsel, R. J. Harrison, and D. A. Dixon, "Multireference configuration interaction calculations on cr2: passing the one billion limit in mrci/mracpf calculations," *The Journal of Physical Chemistry A*, vol. 103, no. 1, pp. 152–155, 1999.

[39] D. Michalopoulos, M. Geusic, S. Hansen, D. Powers, and R. Smalley, "The bond length of chromium dimer," *The Journal of Physical Chemistry*, vol. 86, no. 20, pp. 3914–3916, 1982.

[40] Z. hui Yang, M. R. Pederson, and J. P. Perdew, "Full self-consistency in the fermi-orbital self-interaction correction," *Physical Review A*, vol. 95, may 2017.

Vita

Gustavo Bravo started his studies in physics at the Universidad de Sonora in the fall of 2015, where he was a member of multiple laboratories and research groups, being in charge of computational or experimental tasks. In 2020 he graduated with honors and received a bachelor of science in physics.

He joined the University of Texas at El Paso in the spring of 2021, where he worked as a research assistant for the Molecular Magnetism and Quantum Theory Lab, under the advisory of Dr Mark R. Pederson, and Dr Koblar A. Jackson. His efforts were focused on scientific software development and theoretical physics.

Gustavo Bravo will join Northeastern University's Physic PhD program in the fall of 2023 to continue his formation as a physicist and researcher.